Strong saturation absorption imaging of dense clouds of ultracold atoms

G. Reinaudi, T. Lahaye, 1,2 Z. Wang, 1,3 and D. Guéry-Odelin 1,*

¹Laboratoire Kastler Brossel, Ecole Normale Supérieure, 24 Rue Lhomond, F-75231 Paris Cedex 05, France ²5. Physikalisches Institut, Universität Stuttgart, Pfaffenwaldring 57, D-70550 Stuttgart, Germany ³Department of Physics, Institute of Optics, Zhejiang University, Hangzhou 310027, China *Corresponding author: dgo@lkb.ens.fr

> Received July 30, 2007; revised September 13, 2007; accepted September 14, 2007; posted September 27, 2007 (Doc. ID 85479); published October 23, 2007

We report on a far above saturation absorption imaging technique to investigate the characteristics of dense packets of ultracold atoms. The transparency of the cloud is controlled by the incident light intensity as a result of the nonlinear response of the atoms to the probe beam. We detail our experimental procedure to calibrate the imaging system for reliable quantitative measurements and demonstrate the use of this technique to extract the profile and its spatial extent of an optically thick atomic cloud. © 2007 Optical Society of America

OCIS codes: 110.0110, 020.7010.

Recently there has been a resurgent interest in the production of dense samples [1,2] containing a large number of cold neutral atoms with highly compressed magneto-optical traps (MOTs) [3,4]. These studies, combined with optical trapping, opened the way to a simplified and very rapid production of Bose–Einstein condensates [5] and may also play a key role in the production of a cw atom laser based on the periodic coupling of atomic packets into a magnetic guide, yielding a promising starting point for evaporative cooling [6].

For dense clouds, an important issue is the reliability of the method used to extract the atomic densities. The predominant imaging techniques for dilute samples, namely, low-intensity fluorescent and absorption imaging, turn out to be unreliable when probing a dense atomic packet [7,8]. The former critically depends on the value of the illuminating intensity, the frequency, and the repartition of atoms between the different Zeeman sublevels. The latter poses a problem as soon as the optical depth, proportional to the column density of atoms along the probe direction, is of the order of 3 to 4, because of the limited dynamic range of the CCD camera.

It turns out to be difficult to take advantage of the reduced atom-photon cross section of an offresonance probe since the sample behaves like a gradient-index lens in this regime. Alternatively optically thick clouds have been successfully probed with phase contrast imaging [7] and the fluorescence imaging technique in the far above saturation intensity limit [3]. In this latter method, the probe intensity was larger by more than 3 orders of magnitude than the saturation intensity. In this regime, all atoms, independently of their Zeeman sublevel distribution, spend half of the time in the excited state. This method allows one to probe a cloud with a very large optical depth but requires a dramatically high incident intensity and a subtle alignment of the two counterpropagating beams used to drive the fluorescence.

In this Letter, we report on our realization of a robust, accurate, and reliable far above saturation intensity absorption imaging technique aimed at investigating such dense atomic samples, which does not require the use of a powerful laser.

Indeed, in our experiment, the probe light is provided only by diode lasers. A semiconductor slave laser is injection locked to a 0.5 MHz linewidth distributed Bragg reflector (DBR) master diode laser and spatially filtered by a pinhole. The purpose of this arrangement is to benefit from a narrow linewidth probe tuned on the transition $^{87}{\rm Rb},~5^2S_{1/2}{\to}5^2P_{3/2}$ while having a relatively large power (30 mW) available to probe the atoms. An acousto-optic modulator placed before the pinhole is used to produce light pulses as short as 250 ns. The shadow cast by the atoms on the resonant probe beam is imaged on a CCD camera.

The response of the atoms, i.e., the population driven in the excited state by the imaging laser beam, depends on the *effective* saturation intensity $I_{\rm eff}^{\rm sat} = \alpha^* I_0^{\rm sat}$, where $I_0^{\rm sat}$ is the saturation intensity for the corresponding two-level transition $(I_0^{\rm sat})$ =1.67 mW/cm² for ⁸⁷Rb). The dimensionless parameter α^* accounts for corrections due to the polarization of the imaging beam, the structure of the excited state, and the different Zeeman sublevel populations of the degenerate ground state of the optical transition.

To extract the spatial atomic density n(x,y,z) of the cloud, we acquire as usual three images: $I_{\rm w}(x,y)$ with the atoms and probe beam on, $I_{wo}(x,y)$ without the atoms and probe on, and $I_{\text{dark}}(x,y)$ without atoms and probe off. From those images, we work out for each pixel (x,y), the light intensity $I_f(x,y)=I_w(x,y)$ $-I_{\text{dark}}(x,y)$ (resp. $I_{\text{i}}(x,y)=I_{\text{wo}}(x,y)-I_{\text{dark}}(x,y)$) of the imaging beam in the presence (absence) of atoms by removing the contribution of the background light illumination taken in the absence of the detection beam.

The Beer's law in the presence of saturation effect and for a resonant incident light can be recast in the form

$$\frac{\mathrm{d}I}{\mathrm{d}z} = -n \frac{\sigma_0}{\alpha^*} \frac{1}{1 + I/I_{\mathrm{eff}}^{\mathrm{sat}}} I \equiv -n \,\sigma(I)I, \qquad (1)$$

where $\sigma_0=3\lambda^2/2\pi$ is the resonant cross section for a two-level atom and $\sigma(I)$ is the effective cross section including saturation correction. From Eq. (1), one readily obtains the expression for the optical depth:

$$od_0(x,y) \equiv \sigma_0 \int n(x,y,z) dz = f(x,y;\alpha^*), \qquad (2)$$

where $f(x,y;\alpha^*)$ is defined by

$$f(x,y;\alpha^*) = -\alpha^* \ln \left(\frac{I_f(x,y)}{I_i(x,y)} \right) + \frac{I_i(x,y) - I_f(x,y)}{I_0^{\text{sat}}}.$$
 (3)

The optical density is defined by $\delta_0(x,y) = -\ln[I_f(x,y)/I_i(x,y)]$. The definition of $od_0(x,y)$ depends only on the cloud properties. However, to compute this quantity one needs to know α^* .

For low-intensity absorption imaging $[I_i(x,y) \ll I_0^{\rm sat}]$, the optical depth reads $od_0(x,y) \simeq \alpha^* \delta_0(x,y)$. The unknown parameter α^* still needs to be determined independently. The strong saturation imaging technique takes advantage of the reduction of the effective cross section $\sigma(I)$ when $I \gg \alpha^* I_0^{\rm sat}$. In this limit, the optical depth can be inferred from the images if one knows the incident and final intensities $I_i(x,y)$ and not only their ratio as well as the dimensionless parameter α^* [see Eq. (3) and Fig. 1].

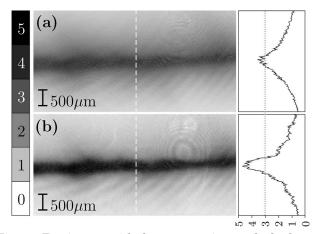


Fig. 1. Two images with the cross section marked taken at the dashed line position of a dense elongated cloud prepared in the same conditions. The transverse profile is given by the dimensionless function $f(x,y;\alpha^*)/\alpha^*$, and the dotted line corresponds to the value 3. (a) Low-intensity absorption imaging. Almost all the light is absorbed in the center of the cloud. The limited dynamic range prohibits the measurement of a too high optical depth. (b) High-intensity absorption imaging. Only the second method shows that the profile has a double structure, with an rms size for the central peak of 300 μ m, corresponding for this example to a peak atomic density $\sim 4(\pm 1) \times 10^{10} \, \text{atoms/cm}^3$ and $\max(od_0) \sim 9$. The two methods coincide in the low optical depth region.

In the context of our far above saturation absorption imaging technique, the absolute calibration just consists of determining the parameter α^* . We proceed in the following manner: the sample of cold atoms is generated by a compressed elongated twodimensional MOT. The cloud is imaged after a not too short time of flight so that its maximum optical density is not too high (~ 2) , which also guarantees the validity of the low-intensity absorption imaging. As the imaging technique is destructive, we acquire several sets of images (typically five) of a cloud always prepared in the same conditions for different incident intensities. In practice, we vary the intensity of the imaging beam by more than 2 orders of magnitude while keeping the number of photons per pulse constant: the duration of the pulse was varied from 250 ns $(I_i \simeq 23 \text{ mW/cm}^2)$ to 100 μ s $(I_i \simeq 23 \text{ mW/cm}^2)$ ~0.06 mW/cm²). Keeping the number of absorbed photons small (~5 photons per atom on average) avoids pushing and heating the cloud.

In order to infer the value of α^* , we calculate, for different values of α ranging from 1 to 4, the function $f(x,y;\alpha)$ for the set of images. We extract the amplitude $od(\alpha)$ of those calculated optical depths using a Gaussian fit. There is only one value α^* of α for which all the calculated $od(\alpha)$ are equal over the whole range of incident intensities. Indeed, od_0 depends only on the atomic cloud characteristics and not on the incident probe intensity [see Eq. (2)]. An example of such a calibration is provided in Fig. 2.

In practice, we infer by a least-squares method the value α^* for which $od(\alpha)$ has a minimum standard deviation over the whole range (more than 2 orders of magnitude) of incident intensities used to image the cloud (see Fig. 2 inset). We find $\alpha^* = 2.12 \pm 0.1$ and a maximum optical depth $od_0 = 4.8$ that corresponds to

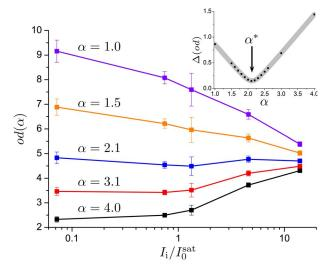


Fig. 2. (Color online) Cloud is imaged using different probe intensities (from $I_0^{\rm sat}/15$ to $15I_0^{\rm sat}$). For each image, the maximum optical depth of the cloud $od(\alpha)$, deduced from a Gaussian fit, is calculated with several values of the unknown parameter α using the function f. The plot represents $od(\alpha)$ as a function of the incoming intensity. The standard deviation $\Delta(od)$ of each set of data points (see inset) exhibits a clear minimum as a function of the parameter α . The minimum of $\Delta(od)$ gives $\alpha^* = 2.12 \pm 0.1$.

an optical density of δ_0 =2.25 as deduced from the low-intensity absorption imaging. We stress that this procedure allows for an absolute determination of the number of atoms, its accuracy being ultimately determined by the knowledge of the incident intensity extracted from each pixel. For this purpose, we use the CCD array that we have first carefully calibrated. To avoid the saturation of the CCD pixels, we use a well-calibrated density filter in front of the camera.

This value for α^* is to be compared with the result of the Bloch equations for the corresponding multiple level system. For our data, the atoms are initially in the $|g\rangle = 5^2 S_{1/2}$, F=2 hyperfine state (fivefold degenerated) and the π -polarized probe is resonant with the $|e\rangle = 5^2 P_{3/2}$, F' = 3 hyperfine excited state (seven-fold degenerated). The probability to excite the $5^2P_{3/2}$, F'=2 is negligible (below 1%). The transition $|g\rangle$ $\rightarrow |e\rangle$ can be considered in this limit as closed. From the numerical integration of the Bloch equations, we find out that (i) the steady state solution is approximately valid even for the shortest pulses that we use, and (ii) the correction factor α^* for the two-level saturation intensity lies in between 1 and 2 depending on the polarization of the probe. Experimentally, the polarization of the beam cannot be perfectly under control because of the slight birefringence of the viewports. In addition, a residual magnetic field may also influence the effective value of α^* .

After calibration, the high-intensity imaging technique is applied to the same cloud but without time of flight. The transparency of the atomic cloud is controlled by the probe intensity. Our numerical studies based on Eqs. (2) and (3) show that the true profile of the cloud can be reliably inferred from the strong saturation absorption images as soon as the incident intensity of the probe beam is of the order of I_i $\sim \max(od_0)I_{\text{eff}}^{\text{sat}}$. Note that this intensity is much less than the one needed for a reliable high-intensity fluorescence imaging technique [3]. We have checked this prediction by imaging with different incident intensities a compressed two-dimensional MOT prepared in the same conditions. To compress the MOT, we proceed in the following manner: the repumper intensity is divided by 15 in 1 ms, the detuning is ramped linearly from -3Γ to -9Γ , and the gradient from 5 to 20 G/cm in 15 ms. Thanks to our imaging technique, we systematically identify a double structure with a central dense region having a maximum peak atomic density of the order of $2(\pm 1) \times 10^{11}$ atoms/cm³ corresponding to $\max(od_0) \sim 45$. Half of the atoms (1.5) $\times 10^8$) remain in the wing. The profile of those wings

and their number of atoms inferred from the low- and high-intensity absorption imaging techniques perfectly coincides.

In addition, this technique is particularly well suited for the estimation of the spatial extent of dense atomic packets with one or more sizes very small ($\Delta x_0 \leq 30~\mu\text{m}$). If T is the temperature of the cloud, the size of the packet reflects the velocity distribution after a time-of-flight duration of the order of $\tau = (m\Delta x_0^2/k_BT)^{1/2}$. For a cloud with an initial size of $10~\mu\text{m}$ and a temperature of $100~\mu\text{K}$, $\tau \sim 100~\mu\text{s}$. By contrast with low-intensity absorption imaging, for which the pulse duration is of the order of the time τ , the very short pulse used for high-intensity imaging prevents heating and permits one to extract the correct profile.

We have demonstrated a high-intensity absorption imaging technique well suited for dense, small-size atomic clouds. This technique is robust against small frequency and intensity variations of the probe and does not require an extremely large probe intensity. We have shown how it can be reliably calibrated exploiting the nonlinear atomic response.

We thank J. Dalibard, T. Kawalec, and A. Couvert for the careful reading of the manuscript. Support for this research came from the Délégation Générale pour l'Armement (DGA) contract number 05-251487 and the Institut Francilien de Recherche sur les Atomes Froids (IFRAF). Z. Wang acknowledges support from the European Marie Curie Grant MIF1-CT-2004-509423, and G. Reinaudi from the DGA.

References

- W. Petrich, M. H. Anderson, J. R. Ensher, and E. A. Cornell, J. Opt. Soc. Am. B 11, 1332 (1994).
- C. G. Townsend, N. H. Edwards, C. J. Cooper, K. P. Zetie, C. J. Foot, A. M. Steane, P. Szriftgiser, H. Perrin, and J. Dalibard, Phys. Rev. A 52, 1423 (1995).
- 3. Marshall T. DePue, S. Luckman Winoto, D. J. Han, and David S. Weiss, Opt. Commun. 180, 73 (2000).
- 4. M. Vengalatorre, R. S. Conroy, and M. G. Prentiss, Phys. Rev. Lett. **92**, 183001 (2004).
- T. Kinoshita, T. Wenger, and D. S. Weiss, Phys. Rev. A 71, 011602 (2005).
- T. Lahaye, J. M. Vogels, K. J. Günter, Z. Wang, J. Dalibard, and D. Guéry-Odelin, Phys. Rev. Lett. 93, 093003 (2004).
- 7. W. Ketterle, D. S. Durfee, and D. M. Stamper-Kurn, Proceedings of the International School of Physics "Enrico Fermi", M. Inguscio, S. Stringari, and C. E. Wieman, eds. (IOS Press, 1999) and references therein.
- S. Kadlecek, J. Sebby, R. Newell, and T. G. Walker, Opt. Lett. 26, 137 (2001).